Journal of Macromolecular Science, Part A
Publication details, including instructions for authors and subscription information:
http://www.informaworld.com/smpp/title~content=t713597274

The Kinetics of Donor-Acceptor Complex Polymerization. II. Applications of the Kinetic Equations

J. Tanner[ab]; J. Rybicky[a]; B. L. Funt[ac]
[a] Department of Chemistry, Simon Fraser University, Vancouver, British Columbia, Canada [b] Petrochemical Polymer Laboratory, Imperial Chemical Industries Ltd., Runcorn, Cheshire, England [c] Department of Chemistry, University of California, San Diego, La Jolla, California

Online publication date: 29 September 2010

To cite this Article Tanner, J. , Rybicky, J. and Funt, B. L.(1972) 'The Kinetics of Donor-Acceptor Complex Polymerization. II. Applications of the Kinetic Equations', Journal of Macromolecular Science, Part A, 6: 2, 241 — 257
To link to this Article: DOI: 10.1080/0022233X.1972.10131855
URL: http://dx.doi.org/10.1080/0022233X.1972.10131855

J. MACROMOL. SCI.—CHEM., A6(2), pp. 241-257

The Kinetics of Donor-Acceptor Complex Polymerization. II. Applications of the Kinetic Equations

J. TANNER,* J. RYBICKY, and B. L. FUNT†

Department of Chemistry
Simon Fraser University
Vancouver, British Columbia, Canada

ABSTRACT

The factors affecting the polymer yield profile in donor-acceptor copolymerization are appraised. Methods for extracting kinetic parameters from the experimental data are outlined and some experimental examples are provided.

In Paper I [1] of this series on the kinetics of donor-acceptor polymerizations, we have derived a series of equations linking polymer yield with time. These equations, because of difficulties in the exact solutions of the various differential rate equations, have been derived for various, particular conditions of initial monomer and catalyst concentrations and for low conversion to polymer.

---

*Present address: Imperial Chemical Industries Ltd., Petrochemical and Polymer Laboratory, P.O. Box 11, The Heath, Runcorn, Cheshire, England.

†Currently Visiting Scientist, Department of Chemistry, University of California, San Diego, La Jolla, California 92037.

Whereas Paper I [1] was intended solely for the development of the rate equations, in the present work we intend to treat the subject from a more practical standpoint. This may be summarized as follows:

A. An appraisal of the equations themselves, particularly with respect to the effect of changes in the kinetic rate parameters on the yield/time relationships.

B. An outline of methods of extracting useful kinetic parameters from experimental data.

C. Some experimental examples using the acrylonitrile (AN), 1.3-butadiene (BD), zinc chloride ($ZnCl_2$), 1.2-dichloroethane (DCE) system and the AN styrene (S), zinc bromide ($ZnBr_2$) DCE system.

The kinetic scheme remains unchanged from Paper I [1], and may be written

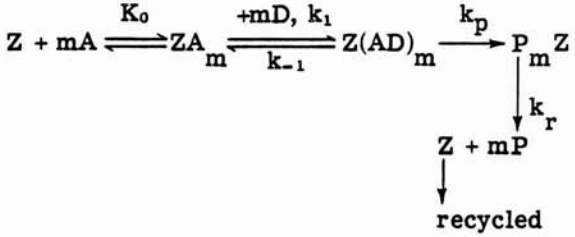

All rate constants, equilibrium constants, and component symbols have the same significance as in Paper I [1] and are described below.

Z:	the free catalyst salt.
A:	the acceptor monomer.
D:	the donor monomer.
ZA_m:	the adduct formed between the acceptor monomer, A, and the catalyst salt, Z, of variable stoichiometry, m.
$Z(AD)_m$:	the donor-acceptor complex of the salt and both monomers of variable stoichiometry, m.
P_mZ:	the catalyst-containing macromolecular product formed from the polymerization of $Z(AD)_m$.
P:	the macromolecular product formed after the regeneration of catalyst from P_mZ.

K_0: equilibrium constant defined as

$$K_0 = ZA_m/ZA^m$$

k_1, k_{-1}: the forward and backward rate constants for the complex formation, respectively.

k_p, k_r: rate constants for the propagation and regeneration reactions, respectively.

In this paper, the concentration conditions for Cases I, II, and III are defined as follows (as in Paper I)

I: $A_0, D_0 \gg Z_0$
II: $A_0, Z_0 \gg D_0$
III: $D_0, Z_0 \gg Z_0$

SECTION A

We will now consider the various possible combinations of reactant concentrations (Cases I, II, and III) in sequence and discuss the effects of the rate parameters on the polymer yield/time relationships.

Case I

The polymer yield/time relationship in Paper I can be written in general as

$$P_t = Et + F(1 - \exp(-C_2t)) \quad (1)$$

The yield of polymer is therefore determined by two time-dependent terms; a linear term and an exponential term. The relative contribution of these two terms to copolymer conversion depends on the magnitudes of E, F, C_2, and time (t). This in turn depends on the relative magnitude of k_p, k_r, k_{-1}, k_1, K_0, A_0, D_0, m, and Z_0. This may be more readily seen when we standardize all constants except k_p and k_r,

the apparent polymer propagation constant and the catalyst regeneration constant, respectively. This is shown in Fig. 1. Curve 1 indicates, in general, $k_r \gg k_p$, Curve 2 indicates $k_p \approx k_r$, and Curve 3 indicates $k_p \gg k_r$. This holds true when the steady-state conditions are met. The forms of the curves are independent of the relative values of k_p and k_{-1} except for the special case when $k_p \gg k_{-1}$. In this case k_p is not rate controlling and the behavior of the system is determined by the relative magnitudes of k_r and k_1.

Figure 2 shows, when over-all k_p is larger than k_r, the effects of varying the ratio of k_p to k_r. Curves 1 through 3 indicate an

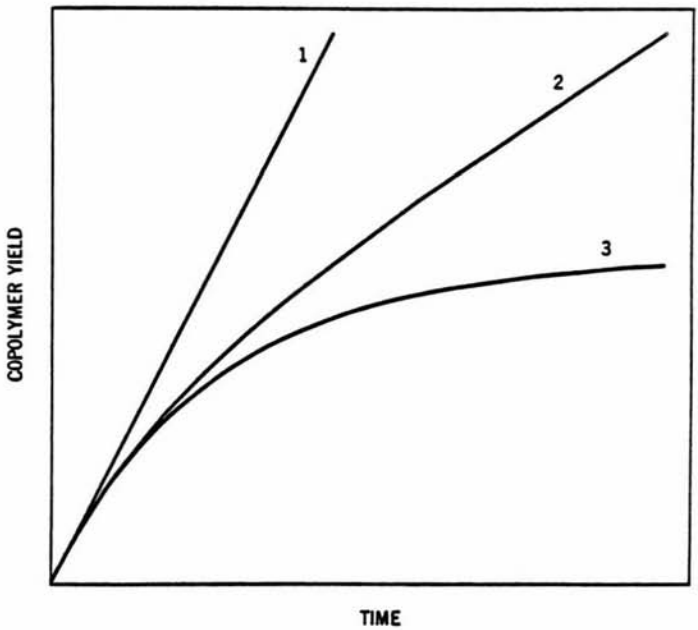

FIG. 1. Curve 1: $k_r \gg k_p$, $k_{-1} \gg k_p$ or $k_r \gg k_1$ when $k_{-1} \ll k_p$. Curve 2: $k_r \sim k_p$, $k_{-1} \gg k_p$ or $k_r \sim k_1$ when $k_{-1} \ll k_p$. Curve 3: $k_r \ll k_p$, $k_{-1} \gg k_p$ or $k_r \ll k_1$ when $k_{-1} \ll k_p$.

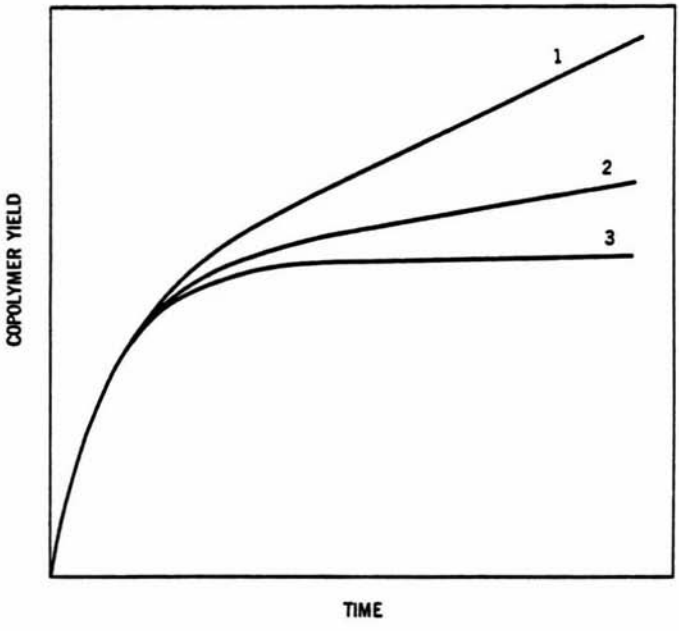

FIG. 2. Curve 1: $k_r < k_p$. Curve 2: $k_r \ll k_p$. Curve 3 $k_r \lll k_p$.

increasing ratio of k_p to k_r. It should also be noted (in Fig. 2) that, as the ratio of k_p to k_r increases, the intercept on the ordinate increases to a limiting value (Curve 3). This value is in fact mZ_0. At the same time the slope of the curve (at high t) tends to zero.

In Fig. 3, again when $k_p \gg k_r$, we see the effect of increasing m, the stoichiometric constant. Curves 1, 2, and 3, each for a fixed value of $k_p \gg k_r$, have values of m = 2.0, 1.5, and 1.0, respectively. The intercepts are approximately in the ratio of the m values (note: the curve origin is set at the point 0,0).

Cases II and III

Because of their similarity, these cases are treated together. In the two cases the catalyst and one of the monomers are in concentration

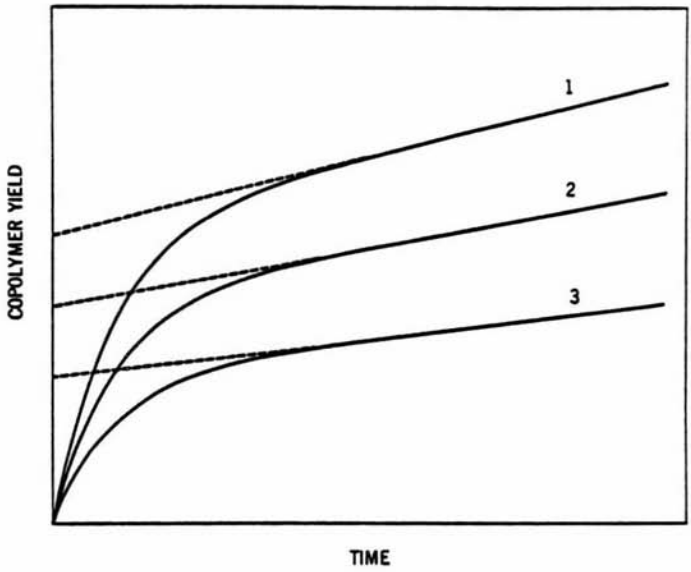

FIG. 3. Curve 1: m = 2.0. Curve 2: m = 1.5. Curve 3: m = 1.0.

excess over the other monomer. The direct result of this is that the final kinetic equations (Eqs. 2 and 3) are independent of k_r, the catalyst regeneration constant.

$$P_t = D_0(1 - \exp(-C_4 t)) \quad \text{(for Case II; Paper I, Eq. 36)} \tag{2}$$

and

$$P_t = A_0(1 - \exp(-C_6 t)) \quad \text{(for Case III; Paper I, Eq. 43)} \tag{3}$$

With the exception of the zero-order case which is linear in P_t and t, a plot of yield of polymer against time gives a smooth curve with a more or less rapid change in rate, depending on the starting concentrations and the rate constant k_p. (However, when $k_p \gg k_{-1}$ the rate becomes independent of k_p and depends primarily upon k_1.)

This behavior is shown in Fig. 4. Curves 1 through 3 indicate decreasing values of k_p. (The curves tend, at infinite time, to a limiting value of polymer conversion, corresponding to D_0 in Case II, and A_0 in Case III. This is not shown, as such a high conversion does not fulfill the condition of integration of the rate equations.) A further point to note here is the possibility, in an experimental situation, of misinterpreting results. When k_p is low, the curve (seen here as Curve 3) is very slight and analysis might suggest, erroneously, a straight line fit.

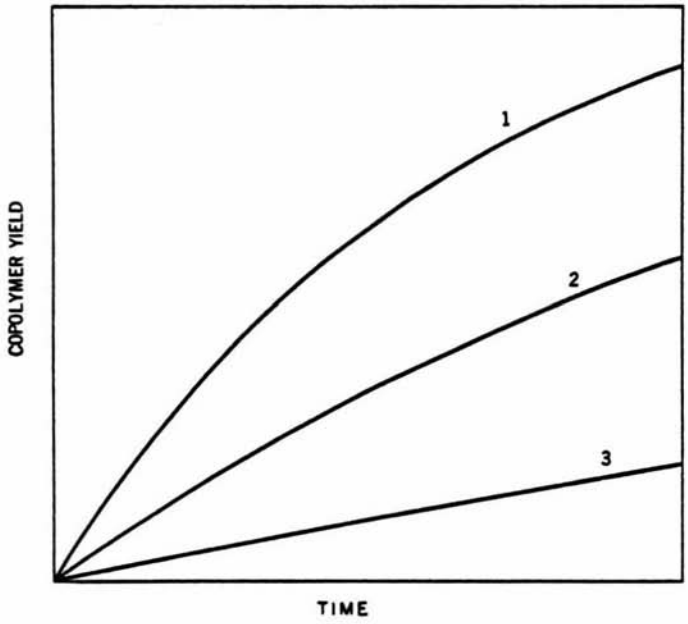

FIG. 4. Curve 1: k_{p_1}. Curve 2: k_{p_2}. Curve 3: k_{p_3}. $k_{p_1} > k_{p_2} > k_{p_3}$.

At this stage it should be stressed that, from an experimental point of view, Case I (A_0, $D_0 \gg Z_0$) is the most desirable and attainable situation, particularly when inorganic salt catalysts are being used (such as zinc halides). This is because of their limited solubility

at all ratios of monomers and solvents and because of very rapid, almost uncontrollable, reactions when high Z_0 is used. It might also be noted that, at high Z_0, the solutions rapidly become very viscous, presumably due to associative interactions between polymer chains [2]. This effect is diminished at low Z_0, or at higher over-all dilution. (However, at high over-all dilution, there is once again a solubility problem with the uncomplexed catalyst when using solvents which have low donicities [3] such as DCE).

SECTION B

The extraction of kinetic information from polymer-yield versus time curves is a simple process involving the following major steps. We will first consider Case I experimental conditions since this is the most easily attainable and the most interesting.

1. Experimental curves are found (at a given set of temperature, solvent, and initiator conditions) for P_t versus t at various values of D_c, the initial donor monomer concentration, still keeping $D_0 \gg Z_0$.
2. These curves are then analyzed mathematically to provide the parameters E, F, and C_2 (see Eq. 1). The actual method of analysis presents some problems since the expression of P_t as a function of t contains one nonlinear parameter ($\exp(-C_2 t)$). This problem is soluble, however, using one of the methods which follow.

(a) Analysis of the curve by a nonlinear least squares method. (These authors have used the FORTRAN IV Program GRIDLS [4], a grid search method with χ^2 minimization, but there are many others from which to choose.)

(b) Curve analysis may also be encompassed by the arbitrary choice of the nonlinear parameter C_2 followed by linear least-squares regression to find E and F. Iteration to minimize χ^2 will provide the best fit and consequently the best values of C_2, E, and F.

(c) The preceeding two methods are general in scope. However, in the special case when $k_p \gg k_r$ (see Fig. 5) it is possible to get good values of the parameters E, F, and C_2 using a two-part linear least-squares regression. In this particular case it would be feasible, if tedious, to hand-calculate.

It is possible to get values of E and F from the linear portion (high t) of the curve (see Fig. 5) using linear least squares curve

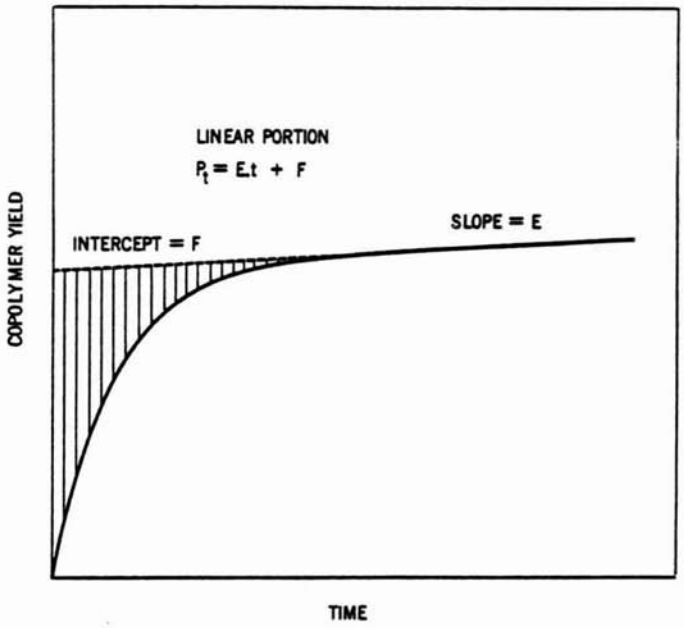

FIG. 5. Analysis of the curve $P_t = Et + F(1 - \exp(-C_2t))$ when $k_p \gg k_r$.

fitting. Then using these values of E and F, it is possible, using the data from the shaded part of the curve, to get a value for C_2 and another value of F).

This can be seen from Eq. (4) where

$$\log (Et + F - (P_t)_t) = \log F - C_2t \qquad (4)$$

Linear least squares (or graphical interpolation) will give a slope of C_2 and an intercept of log F.

3. When E, F, and C_2 have been found for each value of D_0, it is then possible to extract m, k_r, and k_p as detailed in the following sequence of operations.

(a) For each value of D_0 we have E, F, and C_2. For each D_0 value we can then find k_pR, m, and k_r by solving the three simultaneous equations

$$E = mk_pR\left(Z_0 - \frac{C_1}{C_2}\right)$$

$$= mk_pRZ_0\left(1 - \frac{k_pR}{C_2}\right) \tag{5}$$

$$F = \frac{mk_pRC_1}{C_2^2}$$

$$= \frac{m(k_pR)^2 Z_0}{C_2^2} \tag{6}$$

$$C_2 = k_pR + k_r \tag{7}$$

(Eqs. 5, 6, and 7 come from Ref. 1, Eqs. 19, 20, 25, and 26.) Solution of Eqs. (5), (6), and (7) give

$$k_pR = \frac{F.C_2^2}{E + F.C_2} \tag{8}$$

$$m = \frac{FC_2^2}{Z_0}\frac{1}{(k_pR)^2} \tag{9}$$

and

$$k_r = C_2 - k_pR \tag{10}$$

(b) We now have values of k_pR for each value of D_0. We also know m and k_r which are constants. To find k_p, the procedure is

$$R = \frac{QK_0{A_0}^m}{(1 + K_0{A_0}^m)\left(1 + \frac{QK_0{A_0}^m}{1 + K_0{A_0}^m}\right)} \tag{11}$$

and

$$Q = \frac{k_1}{k_{-1} + k_p}\,{D_0}^m \tag{12}$$

(Equations 11 and 12 are shown in Ref. 1, Eqs. 15 and 12.)

Equation (11) may be simplified to

$$R = \frac{Q}{1 + Q} \tag{13}$$

assuming $K_0{A_0}^m \gg 1$.

Then

$$k_pR = \frac{k_pQ}{1 + Q} \tag{14}$$

Substituting for Q, from Equation 12, and rearranging we find

$$\frac{1}{k_pR} = \left(\frac{k_{-1} + k_p}{k_pk_1}\right)\frac{1}{{D_0}^m} + \frac{1}{k_p} \tag{15}$$

Thus, when plotting $1/k_pR$ against $1/{D_0}^m$, the intercept determines k_p.

In Case II (and similarly Case III) once again, the curves of P_t against t are determined experimentally for different D_0's. We have

$$P_t = D_0(1 - \exp(-C_4 t)) \tag{16}$$

and

$$C_4 = \frac{k_p S}{1 + S} \tag{17}$$

and

$$S = \frac{k_1}{k_{-1} + k_p} ZA_0 \tag{18}$$

(See Ref. 1, Eqs. 36, 35, and 28.)

Experimentally, it is possible, by a straightforward least-squares analysis of each curve, to find C_4 for each D_0. Then Eqs. (17) and (18) may be combined and rearranged to give

$$\frac{1}{C_4} = \left(\frac{k_{-1} + k_p}{k_p k_1} \right) \frac{1}{ZA_0} + \frac{1}{k_p} \tag{19}$$

Thus a plot of $1/C_4$ against $1/ZA_0$ yields an intercept determining k_p (ZA_0 is equivalent to A_0 or Z_0 depending which is in lesser amount. This is because the (K_0) equilibrium lies heavily on the right-hand side).

The assumption is made in the foregoing treatment that variation in D_0 does not affect any of the rate constants. This is questionable as, for instance, the dielectric constant will change with D_0.

SECTION C

In this section we have chosen two series of results using different systems. Series I concerns the "spontaneous" or thermally initiated copolymerization of the AN/BD/$ZnCl_2$ system in DCE solvent. Series II concerns the AIBN initiated AN/S/$ZnBr_2$ system, again in DCE as solvent.

Experimental Details

Chemicals

$ZnCl_2$ was dried in vacuo for approximately 50 hr. $ZnBr_2$ was used as supplied without further drying. AN was dried for several days over calcium hydride, CaH_2, and eluted through an alumina column prior to distillation at reduced pressure. S was dried over CaH_2 and distilled at reduced pressure. BD (99.6% instrument grade) was used without further purification. DCE was dried for several weeks over phosphorus pentoxide and distilled under reduced pressure.

All distillations were performed on a spinning-band column of high efficiency. Center cuts (60%) were used in the experiments, the remainder being rejected.

All liquid components were stored under nitrogen or argon before use.

Experimental Procedures

Series I

Using an apparatus similar to that described in an earlier paper [5], a stirred thermostatted polymerization vessel was dosed with $ZnCl_2$, AN, and DCE and degassed. A known amount of BD was added to the vessel and the system was isolated. The temperature of the cell was raised to the polymerization temperature and the time of onset of polymerization was taken when the solution became slightly cloudy. (Polymerization in the system was heterogeneous at all concentrations. In no case was the inhibition period in excess of 2 min.) At the end of the polymerization the polymer and solution were passed into methanol solution. Aqueous ammonia was added, and the polymer was filtered off and dried to constant weight.

Series II

These runs were performed in dilatometers (200 ml volume, stirred) in constant temperature baths. The solution level in the capillary tube was followed with a cathetometer. Precalculated

amounts of the reaction components were added to the dilatometers and the solutions were degassed on a vacuum line. The dilatometers were sealed off, put into a constant temperature bath, and allowed to come to the polymerization temperature. There was a small inhibition period (10 min) prior to the onset of polymerization. In solutions containing low A_0/D_0 ratios, the polymerizations were heterogeneous and the onset of polymerization was noted visually. For the purposes of this publication, the inhibition period was not studied and t_0 was taken as being at the onset of polymerization. Conversion was measured by precipitating the polymer solution as before and drying to constant weight.

In both series, polymer compositions were found to be those of 1:1 copolymers, within experimental error, using elemental analysis or IR analysis [2].

Results

Figure 6 shows the BD/AN/$ZnCl_2$ system (Series I) in concentration conditions comparable to the Case I situation (where BD_0, $AN_0 \gg (ZnCl_2)_0$). The line drawn through the points in the Fig. 6 was calculated using curve-fitting techniques to the theoretical equation (Eq. 1) which describes these conditions.

Figure 7 shows the S/AN/$ZnBr_2$ system (Series II), once again in concentration conditions comparable to the Case I situation (where S_0, $AN_0 \gg (ZnBr_2)_0$). For the sake of representational clarity every other point has been omitted from the curves. In both experiments shown in Fig. 7 (Curves 1 and 2) the amount of zinc bromide catalyst and the amount of AIBN (azobisisobutyronitrile) were kept constant and only the ratio of S to AN was altered (S + AN = 2 moles/liter). This shows that a simple alteration of the ratio of the reactants, while still upholding the conditions of Case I, can drastically alter the shape of the curves. This may be explained in this case (with passing reference to Fig. 1) by supposing that when there is more AN, k_r, the catalyst regeneration constant, is increased relative to k_p, the apparent propagation constant, (Curve 2). When there is less AN (Curve 1) it is possible that k_r is not so large and, in fact, a two-part rate curve (compare with Fig. 6) will occur. However, this is undoubtedly not the whole picture, since dielectric changes will also be affecting all the constants.

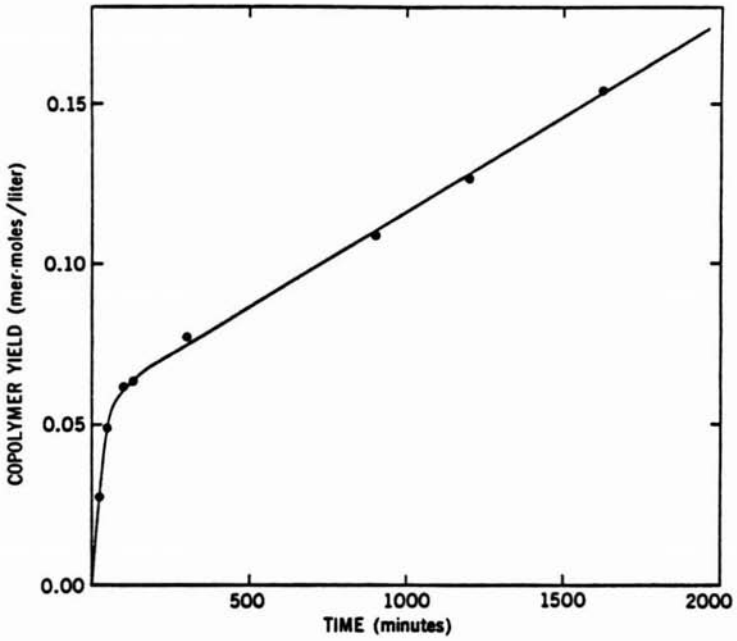

FIG. 6. $ZnCl_2$ (3.87×10^{-2} mole/liter), AN (1.98 mole/liter), BD (0.74 mole/liter), DCE (37 g). Temperature 60°C. Elementary analysis of the products showed 49-52% of AN units through the whole polymerization run. The constants for the solid line (see (Eq. 1): $E = 5.85 \times 10^{-5}$ moles liter^{-1} min^{-1}; $F = 5.73 \times 10^{-2}$ moles liter^{-1}; $C_2 = 3.34 \times 10^{-2}$ min^{-1}.

Discussion

The experimental curves (Figs. 6 and 7) which are presented here have not been numerically analyzed (see Section B) since there is insufficient data to present a complete estimation of the rate constants. In subsequent papers we will show the complete kinetic analysis of these two systems according to the theories and methods devised in this paper (and in Paper I).

Since the experimental conditions required for this kinetic treatment to be valid are quite restrictive, there is very little work in the literature with which to compare our experimental and

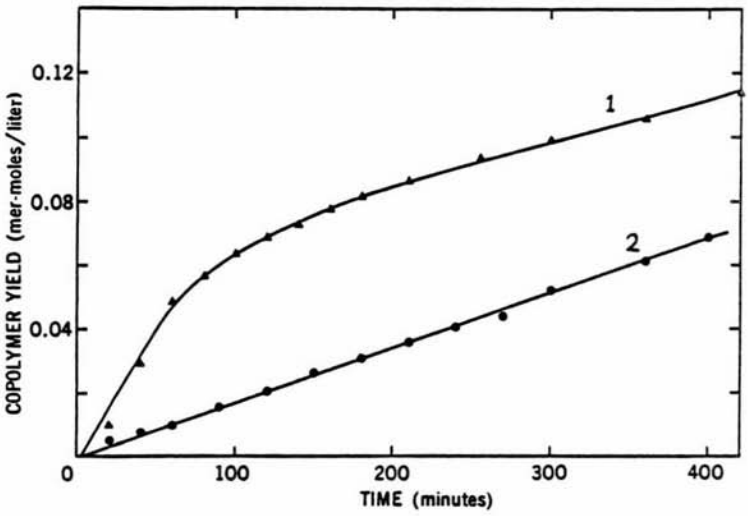

FIG. 7. Curve 1: $ZnBr_2$ (3.00×10^{-2} mole/liter), AN (0.410 mole/liter), styrene (1.62 mole/liter), DCE (total volume of system, 208 ml), AIBN (5×10^{-3} mole/liter), temperature 40°C. Curve 2: $ZnBr_2$ (3.00×10^{-2} mole/liter), AN (1.64 mole/liter), styrene (0.41 mole/liter), DCE (total volume of system, 208 ml), AIBN (5×10^{-3} mole/liter), temperature 40°C.

theoretical findings. A paper by Gaylord and Patnaik [6], using ethyl aluminum sesquichloride in place of zinc halide as catalyst, and with AN and S as the monomers, is the only work of which the authors are aware which fulfills any of our conditions. In this example, Case I conditions are met (AN, S $\gg$ $AlEt_{1.5}Cl_{1.5}$ in the ratios AN:S = 1 and AN:aluminum = 10).

The authors would like to stress that these kinetics are not intended to disprove or prove any of the many theories which have been put forward to explain the donor-acceptor copolymerization phenomenon. They hope, however, that the foregoing treatment might provide a basis for a rigorous numerical rationalization which might itself give some order to an already confused mass of disparate data.

ACKNOWLEDGMENTS

The authors would like to thank Robert Ferguson of this department for assistance with some of the computational aspects of this work. The dilatometric experiments were performed by Mr. Victor Verigin. The financial assistance of the National Research Council of Canada is gratefully acknowledged.

REFERENCES

[1] J. Rybicky, J. Tanner, and B. L. Funt, J. Macromol. Sci.—Chem., A6, 223 (1972).
[2] I. McGregor, Unpublished Results, This Laboratory.
[3] V. Guttman, Chem. Brit., 7, 102 (1971).
[4] P. R. Bevington, Data Reduction and Error Analysis for the Physical Sciences, McGraw-Hill, New York, 1969.
[5] B. L. Funt and J. Rybicky, J. Polym. Sci., Part A-1, 9, 1441 (1971).
[6] N. G. Gaylord and B. Patnaik, J. Polym. Sci., Part B, 8, 411 (1970).

Accepted by editor October 1, 1971
Received for publication October 28, 1971